



Supplement of

Sulfate formation during heavy winter haze events and the potential contribution from heterogeneous $\text{SO}_2 + \text{NO}_2$ reactions in the Yangtze River Delta region, China

Ling Huang et al.

Correspondence to: Li Li (lily@shu.edu.cn) and Cheng Huang (huangc@saes.sh.cn)

The copyright of individual parts of the supplement might differ from the CC BY 4.0 License.

Model performances of nitrate and ammonium concentrations

In addition to sulfate, we also look at modeled nitrate and ammonium concentrations under different scenarios; associated model performance metrics are summarized in Table S7 and S8. For the base case scenario, nitrate and ammonium concentrations were underestimated by 20 %. When only polluted period is considered, underestimation almost doubled to 36 % and 41 % for nitrate and ammonium, respectively. Doubling ammonia emissions results in higher nitrate concentrations simply because more ammonia becomes available to form nitrate. This reduces nitrate underestimation substantially during polluted period from -42 % to -20 % but also leads to even higher nitrate overestimation during clean and transition periods. The impact of the $\text{SO}_2 + \text{NO}_2$ heterogeneous reactions on nitrate formation, on the other hand, is more complicated. With the base case ammonia emissions, predicted nitrate concentrations show negligible changes with the implementation of the heterogeneous reactions. However, with doubled ammonia emissions, predicted nitrate formation is enhanced by $0.3\text{--}1.1 \mu\text{g m}^{-3}$ (noHet_2NH₃ vs. Het_2NH₃). Response of simulated nitrate concentrations to the $\text{SO}_2 + \text{NO}_2$ heterogeneous reactions, in other words, to increased sulfate concentrations, could be affected by two opposing factors. At one hand, nitrate concentrations decrease due to replacement by enhanced formation of sulfate. On the other hand, nitrate formation could be enhanced with more effective hydrolysis of N₂O₅ on sulfate aerosols (Hallquist et al., 2003). A most recent study by Vasilakos et al. (2018) discussed the nitrate substitution paradox with less sulfate and concludes that this paradox is attributable to positive bias in model simulated aerosol pH. Nevertheless, compared with doubled ammonia emissions, the heterogeneous reactions only had small impact on modeled nitrate concentration.

For ammonium, doubling ammonia emissions also leads to higher simulated ammonium concentrations but to a less extent compared with nitrate. Under-prediction of ammonium under polluted conditions is reduced from 41 % in the base case to 31 % in the noHet_2NH₃ scenario. With the base case ammonia emissions, adding the $\text{SO}_2 + \text{NO}_2$ heterogeneous reactions leads to slight increase in ammonium concentrations. When ammonia emissions are doubled, the heterogeneous reactions substantially improve modeled ammonium concentrations. Overall MB of ammonium in scenario Het_2NH₃ is only $-0.4 \mu\text{g m}^{-3}$ (NMB of -3 %) and under-prediction during polluted period is reduced to 24 % in the Het_2NH₃

scenario (from 41 % in the base case scenario). These results suggest that both the heterogeneous reactions as well as sufficient ammonia emissions are needed to improve model simulation of ammonium concentrations.

Model performance of PM_{2.5} concentrations

In the base case scenario, PM_{2.5} concentrations are underestimated by 36 % at the SAES site during polluted periods (Table S9). With doubled ammonia emissions, PM_{2.5} under-prediction is reduced to 30 % during polluted periods, resulting an overall NMB of -2 %. PM_{2.5} concentrations do not change much with the heterogeneous reactions when ammonia emissions are at base case level. With doubled ammonia emissions, concentrations of all three inorganic species are enhanced with the heterogeneous reactions; thus under-prediction of PM_{2.5} during polluted periods in scenario Het_2NH₃ is further reduced to 26 % and the overall NMB is only 1 %. The maximum of simulated PM_{2.5} concentration increases from 460.6 $\mu\text{g m}^{-3}$ in the base scenario to 531.6 $\mu\text{g m}^{-3}$ in scenario Het_2NH₃ (increase by 15 %), which compares well with observed maximum value of 540.3 $\mu\text{g m}^{-3}$.

References

Hallquist, M., Stewart, D. J., Stephenson, S. K., and Cox, R. A.: Hydrolysis of N₂O₅ on sub-micron sulfate aerosols, *Physical Chemistry Chemical Physics.*, 5, 3453-3463. doi:10.1039/B301827J, 2003.

Vasilakos, P., Russell, A., Weber, R., and Nenes, A.: Understanding nitrate formation in a world with less sulfate, *Atmospheric Chemistry and Physics*, 18, 12765-12775, doi: 10.5194/acp-18-12765-2018, 2018.

Table S1. Summary of parameters representing clean, transition, and polluted conditions during Beijing 2015. Temperature (T) and relative humidity (RH) are directly adopted from Table S2 of Wang et al. (2016). NO₂ concentrations are assumed to be 50 % of NOx. Liquid water content (LWC) and aerosol pH are calculated by ISORROPIA assuming a metastable aerosol in CAMx.

Conditions	Temperature [K]	RH [%]	NO ₂ (g) [ppb]	LWC [$\mu\text{g m}^{-3}$]	Aerosol pH [-]
Clean	273.4	21	32	1.24	5.5
Transition	274.4	41	58	12.3	4.2
Polluted	273.9	56	45.5	35.8	4.1

Table S2. Statistical summary of monthly PM_{2.5} simulated from noHet and Het_2NH₃ scenarios at 23 monitoring sites in Zhejiang, Jiangsu and Anhui province during 1 to 29 December 2013.

No.	Province	City	Latitude	Longitude	Observed mean	noHet				Het_2NH ₃			
						Modeled mean	MB	NMB	IOA	Modeled mean	MB	NMB	IOA
1		Hangzhou	29.64	119.03	66.5	60.1	-6.4	-10%	0.74	74.0	7.5	11%	0.75
2		Ningbo	29.85	121.52	153.0	108.9	-44.1	-29%	0.71	122.5	-30.5	-20%	0.78
3		Wenzhou	28.02	120.67	86.6	56.5	-30.1	-35%	0.71	69.3	-17.3	-20%	0.75
4		Jiaxing	30.76	120.76	131.9	102.5	-29.5	-22%	0.73	116.5	-15.4	-12%	0.80
5		Huzhou	30.86	120.09	189.3	119.8	-69.6	-37%	0.67	140.6	-48.7	-26%	0.77
6	Zhejiang	Quzhou	28.94	118.87	71.4	82.8	11.4	16%	0.72	89.8	18.5	26%	0.66
7		Zhoushan	30.02	122.12	99.0	59.5	-39.5	-40%	0.67	72.2	-26.8	-27%	0.75
8		Taizhou	28.65	121.42	106.9	75.3	-31.7	-30%	0.76	88.8	-18.2	-17%	0.82
9		Lishui	28.45	119.91	91.0	61.5	-29.5	-32%	0.62	75.1	-15.9	-17%	0.68
10		Shaoxing	30.01	120.58	198.7	138.8	-60.0	-30%	0.64	166.1	-32.6	-16%	0.72
11		Jinhua	29.11	119.65	164.3	88.2	-76.1	-46%	0.59	105.5	-58.8	-36%	0.68
12		Nanjing	32.01	118.74	170.5	139.4	-31.1	-18%	0.76	152.5	-18.0	-11%	0.80
14		Xuzhou	34.28	117.29	142.0	139.5	-2.4	-2%	0.70	150.0	8.0	6%	0.71
15		Changzhou	31.76	120.00	144.9	127.1	-17.8	-12%	0.83	141.8	-3.1	-2%	0.86
16		Suzhou	31.25	120.56	154.8	119.3	-35.5	-23%	0.74	132.7	-22.1	-14%	0.79
17		Nantong	31.93	120.94	132.1	92.9	-39.2	-30%	0.73	104.3	-27.8	-21%	0.78
18	Jiangsu	Huai'an	33.60	119.04	200.1	109.7	-90.4	-45%	0.55	120.5	-79.6	-40%	0.57
19		Yancheng	33.37	120.13	145.1	130.8	-14.3	-10%	0.75	140.2	-4.9	-3%	0.76
20		Yangzhou	32.38	119.39	144.9	137.6	-7.3	-5%	0.75	149.7	4.8	3%	0.77
21		Zhenjiang	32.21	119.43	143.5	140.7	-2.7	-2%	0.78	154.1	10.7	7%	0.79
22		Taizhou	32.49	119.90	158.0	119.1	-39.0	-25%	0.73	126.9	-31.2	-20%	0.77
23		Suqian	33.95	118.29	139.9	115.9	-24.0	-17%	0.74	126.4	-13.5	-10%	0.74
24	Anhui	Hefei	31.91	117.16	132.2	115.0	-17.1	-13%	0.77	126.8	-5.4	-4%	0.77

Table S3. Statistic summary of WRF simulated meteorological parameters during December 2013 at Pudong and Hongqiao airport monitoring site.

Meteorological parameter	Statistics metric	Pudong	Hongqiao
Temperature [°C]	NMB	0.37	0.01
	NME	0.41	0.16
	IOA	0.86	0.98
Relative humidity [%]	NMB	0.00	0.01
	NME	0.16	0.14
	IOA	0.85	0.92
Wind speed [m s ⁻¹]	NMB	0.33	0.14
	NME	0.42	0.29
	IOA	0.79	0.89
Wind direction [degree]	NMB	-0.36	-0.27

Table S4. Statistical analysis of base case model performance

Species	Observed mean [$\mu\text{g m}^{-3}$] [*]	Modeled mean [$\mu\text{g m}^{-3}$] [*]	MB	NMB	IOA
O ₃	20.1	13.5	-6.6	-33%	0.76
NO ₂	71.5	67.7	-3.8	-5%	0.79
SO ₂	62.9	42.9	-20.0	-32%	0.57
NH ₃	7.4	2.4	-5.0	-68%	0.53
PM _{2.5}	118.7	106.7	-12.0	-10%	0.78
sulfate	17.2	14.5	-2.7	-16%	0.80
ammonium	12.7	9.7	-3.0	-21%	0.79
nitrate	24.4	19.6	-4.8	-20%	0.77
EC	4.3	2.9	-1.4	-32%	0.72
OC	18.7	9.6	-9.1	-49%	0.60

^{*}Units for all species except NH₃ are $\mu\text{g m}^{-3}$; unit for NH₃ is ppb.

Table S5. Statistical metrics of sulfate for different scenarios at SAES site during 1 to 29 December 2013

Scenario	Period	Mean observed sulfate [$\mu\text{g m}^{-3}$]	Mean modeled sulfate [$\mu\text{g m}^{-3}$]	MB [$\mu\text{g m}^{-3}$]	NMB [-]	IOA [-]
noHet	all	17.2	14.4	-2.8	-16%	0.80
	clean	6.7	7.8	1.1	16%	0.68
	transition	14.2	14.7	0.5	4%	0.63
	polluted	36.1	23.1	-13.0	-36%	0.59
Het	all	17.2	15.1	-2.1	-12%	0.83
	clean	6.7	8.0	1.2	18%	0.65
	transition	14.2	15.3	1.2	8%	0.62
	polluted	36.1	24.6	-11.5	-32%	0.63
noHet_2NH ₃	all	17.2	15.2	-2.1	-12%	0.83
	clean	6.7	8.6	1.9	28%	0.65
	transition	14.2	15.0	0.8	6%	0.63
	polluted	36.1	24.5	-11.6	-32%	0.64
Het_2NH ₃	all	17.2	17.0	-0.2	-1%	0.86
	clean	6.7	9.1	2.3	34%	0.59
	transition	14.2	16.3	2.1	15%	0.58
	polluted	36.1	29.1	-6.9	-19%	0.72

Table S6. Observed sulfate and PM_{2.5} concentrations and statistical metrics of sulfate during selected episodes

No. Episode	EP1 12/5 13:00 - 12/7 2:00	EP2 12/9 5:00 - 12/9 14:00	EP3 12/20 0:00 - 12/20 20:00	EP4 12/26 4:00 - 12/26 16:00
Mean observed sulfate [$\mu\text{g m}^{-3}$]	51.2	58.2	36.2	51.3
Mean observed PM _{2.5} [$\mu\text{g m}^{-3}$]	379.9	242.0	186.2	287.4
Max observed sulfate [$\mu\text{g m}^{-3}$]	81.2	93.4	48.6	69.7
[SO_4^{2-}]/[SO_2]	0.52	0.70	0.17	0.19
Mean modeled sulfate [$\mu\text{g m}^{-3}$]	31.3	35.6	10.1	33.4
MB [$\mu\text{g m}^{-3}$]	-19.8	-22.6	-26.2	-21.8
NMB	-39%	-39%	-72%	-46%
IOA	0.46	0.53	0.25	0.54

Table S7. Statistical metrics of nitrate for different scenarios at SAES site during 1 to 29 December 2013

Scenario	Period	Mean observed nitrate [$\mu\text{g m}^{-3}$]	Mean modeled nitrate [$\mu\text{g m}^{-3}$]	MB [$\mu\text{g m}^{-3}$]	NMB [-]	IOA [-]
noHet	all	24.4	19.6	-4.8	-20%	0.77
	clean	9.6	12.0	2.4	25%	0.74
	transition	22.0	20.8	-1.2	-5%	0.76
	polluted	48.4	28.3	-20.1	-42%	0.62
Het	all	24.4	19.6	-4.8	-20%	0.77
	clean	9.6	12.1	2.5	26%	0.73
	transition	22.0	20.9	-1.1	-5%	0.75
	polluted	48.4	28.1	-20.2	-42%	0.62
noHet_2NH ₃	all	24.4	26.8	2.3	10%	0.82
	clean	9.6	15.9	6.3	66%	0.55
	transition	22.0	28.7	6.7	31%	0.56
	polluted	48.4	38.9	-9.5	-20%	0.72
Het_2NH ₃	all	24.4	27.4	2.9	12%	0.83
	clean	9.6	16.2	6.6	69%	0.55
	transition	22.0	29.3	7.3	33%	0.57
	polluted	48.4	40.0	-8.4	-17%	0.75

Table S8. Statistical metrics of ammonium for different scenarios at SAES site during 1 to 29 December 2013

Scenario	Period	Mean observed ammonium [$\mu\text{g m}^{-3}$]	Mean modeled ammonium [$\mu\text{g m}^{-3}$]	MB [$\mu\text{g m}^{-3}$]	NMB [-]	IOA [-]
noHet	all	12.7	10.1	-2.6	-21%	0.79
	clean	4.9	5.8	0.9	19%	0.80
	transition	11.0	10.5	-0.4	-4%	0.76
	polluted	26.2	15.4	-10.8	-41%	0.61
Het	all	12.7	10.4	-2.4	-19%	0.80
	clean	4.9	5.9	1.0	20%	0.79
	transition	11.0	10.8	-0.2	-1%	0.77
	polluted	26.2	15.9	-10.3	-39%	0.63
noHet_2NH ₃	all	12.7	11.6	-1.2	-9%	0.84
	clean	4.9	6.4	1.6	32%	0.70
	transition	11.0	12.0	1.1	10%	0.66
	polluted	26.2	18.1	-8.1	-31%	0.68
Het_2NH ₃	all	12.7	12.4	-0.4	-3%	0.87
	clean	4.9	6.6	1.8	36%	0.70
	transition	11.0	12.6	1.7	15%	0.67
	polluted	26.2	20.0	-6.2	-24%	0.75

Table S9. Statistical metrics of PM_{2.5} for different scenarios at SAES site during 1 to 29 December 2013

Scenario	Period	Mean observed PM _{2.5} [$\mu\text{g m}^{-3}$]	Mean modeled PM _{2.5} [$\mu\text{g m}^{-3}$]	MB [$\mu\text{g m}^{-3}$]	NMB [-]	IOA [-]
noHet	all	118.7	106.7	-12.0	-10%	0.78
	clean	52.8	69.4	16.6	31%	0.73
	transition	103.1	112.9	9.7	9%	0.74
	polluted	232.3	149.2	-83.0	-36%	0.63
Het	all	118.7	107.7	-11.0	-9%	0.79
	clean	52.8	69.8	16.9	32%	0.73
	transition	103.1	113.9	10.8	10%	0.74
	polluted	232.3	151.2	-81.0	-35%	0.64
noHet_2NH ₃	all	118.7	116.0	-2.7	-2%	0.80
	clean	52.8	74.8	22.0	42%	0.68
	transition	103.1	122.5	19.3	19%	0.67
	polluted	232.3	163.7	-68.5	-30%	0.66
Het_2NH ₃	all	118.7	119.4	0.7	1%	0.82
	clean	52.8	75.7	22.9	43%	0.68
	transition	103.1	125.1	22.0	21%	0.68
	polluted	232.3	171.7	-60.6	-26%	0.71

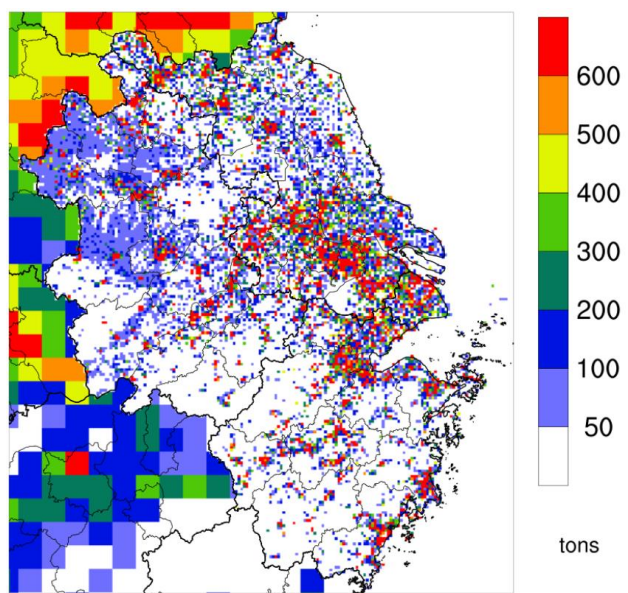


Figure S1 Spatial distribution of primary sulfate emissions (tons) over the 4 km domain during December 2013 (for emissions outside the YRD region, emissions from the MEIC inventory with a spatial resolution of 36 km was used).

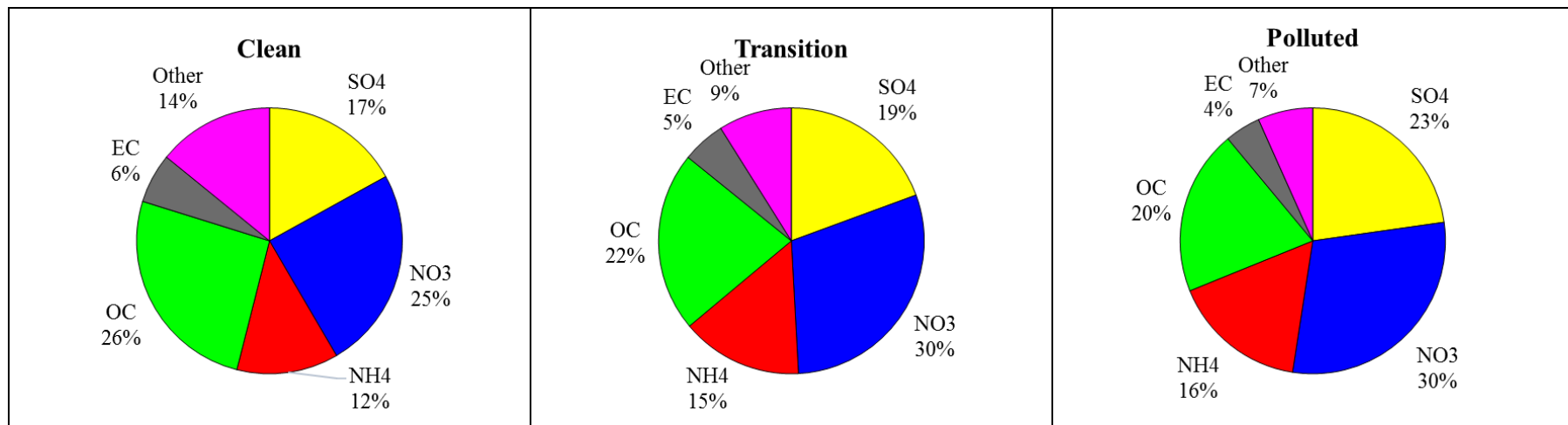


Figure S2. Mass fractions of major PM species for clean, transition, and polluted periods during 1 to 29 December 2013 at SAES site.

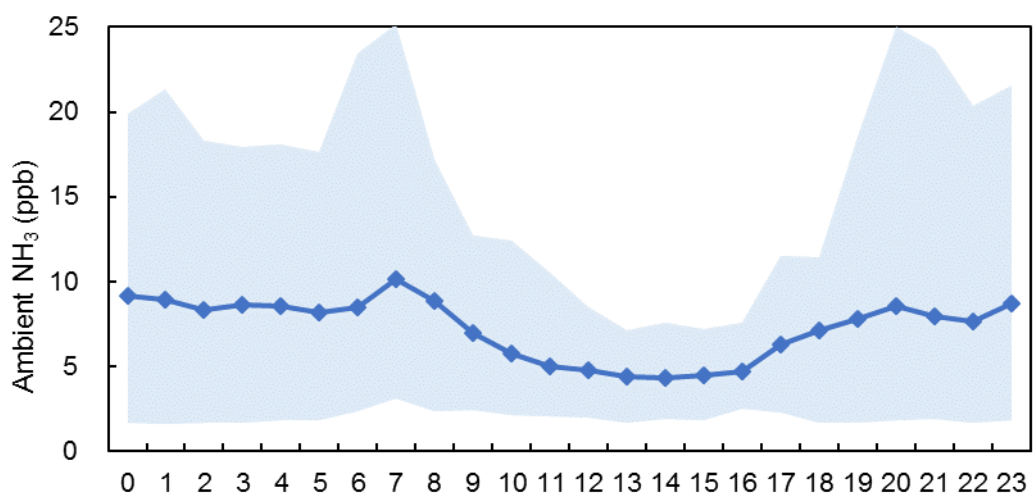


Figure S3. Diurnal profiles of ammonia concentrations (ppb) at FDU site during 1 to 29 December 2013. Shaded areas constrain maximum and minimum concentrations.

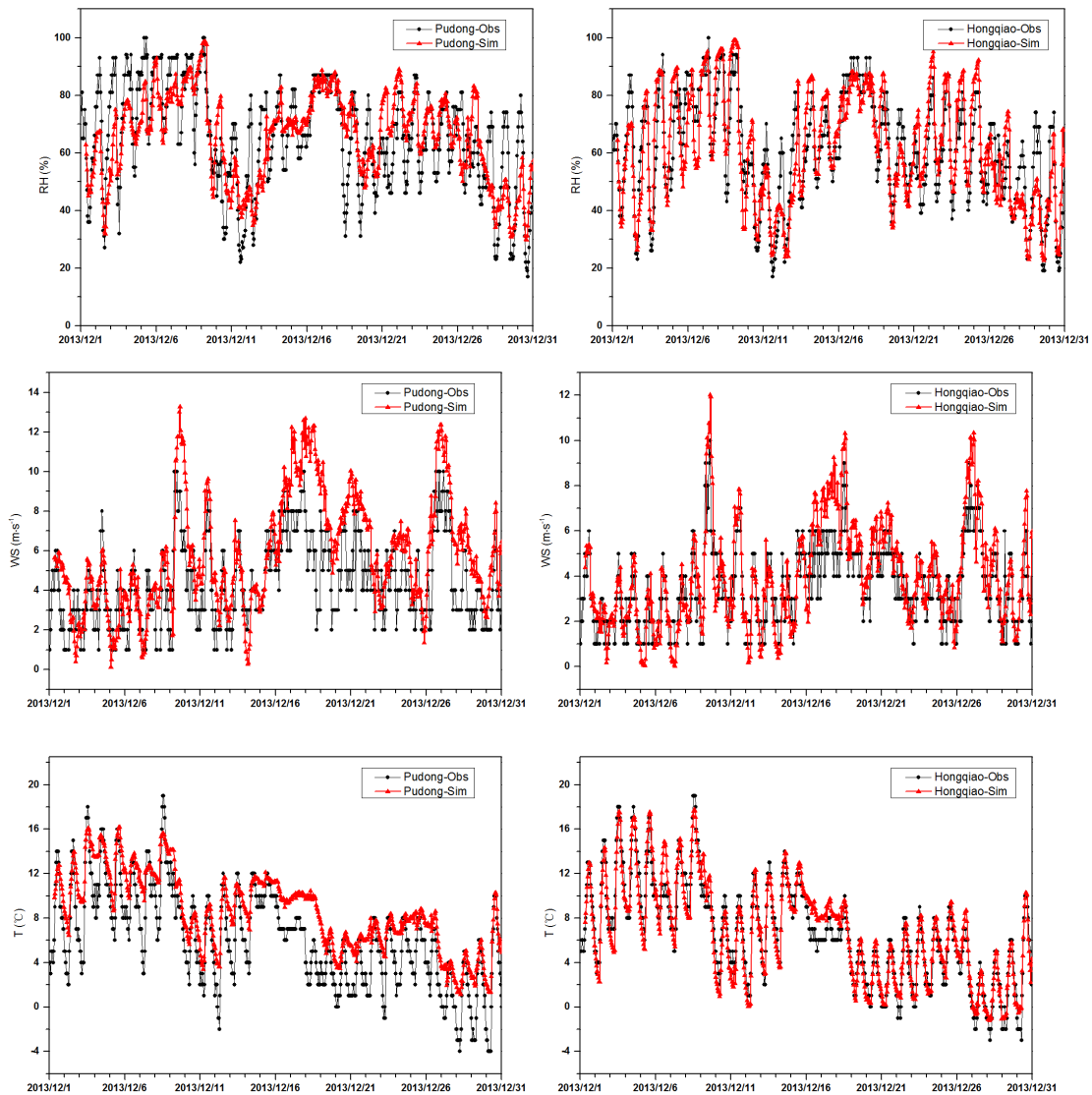
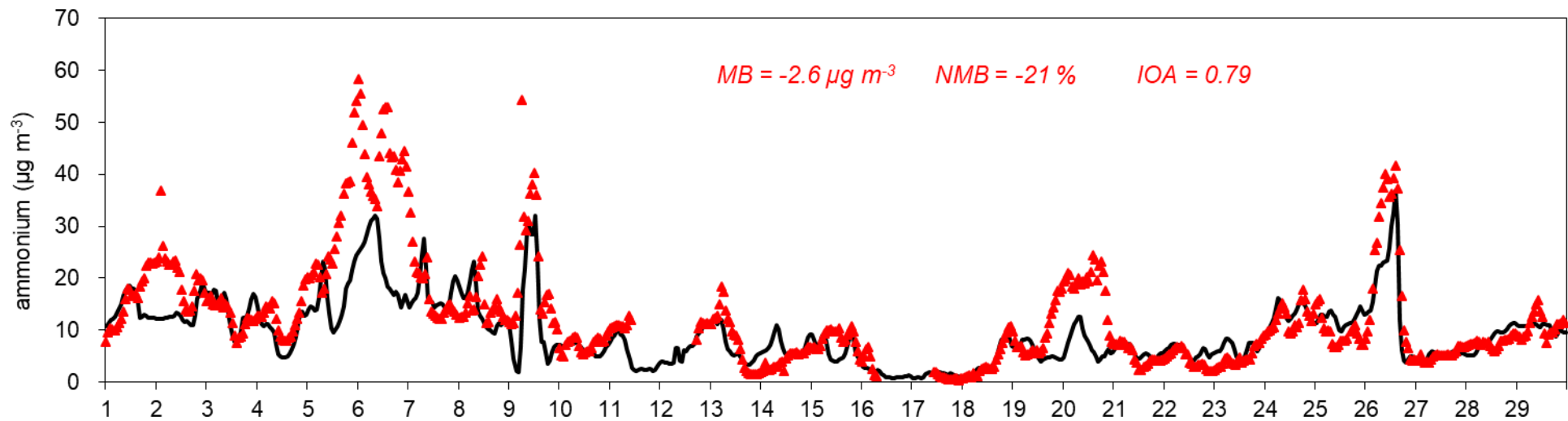
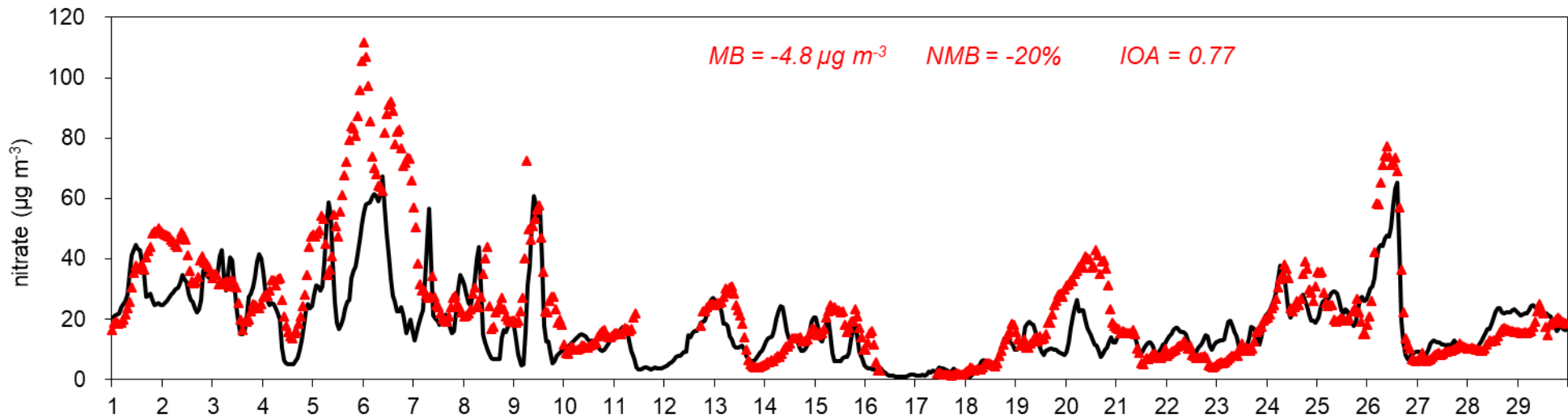
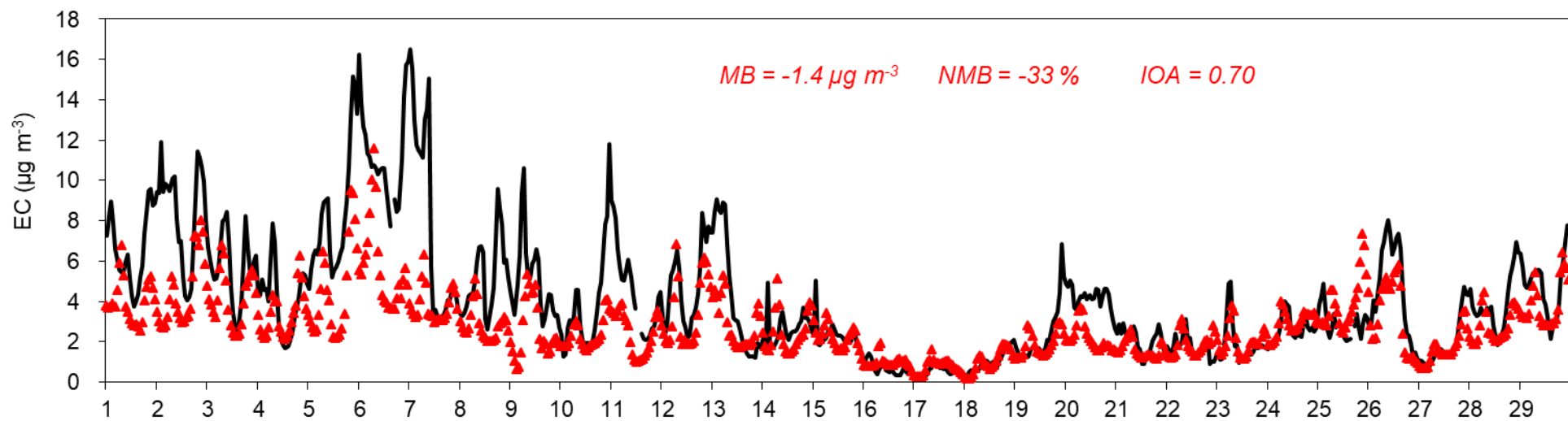
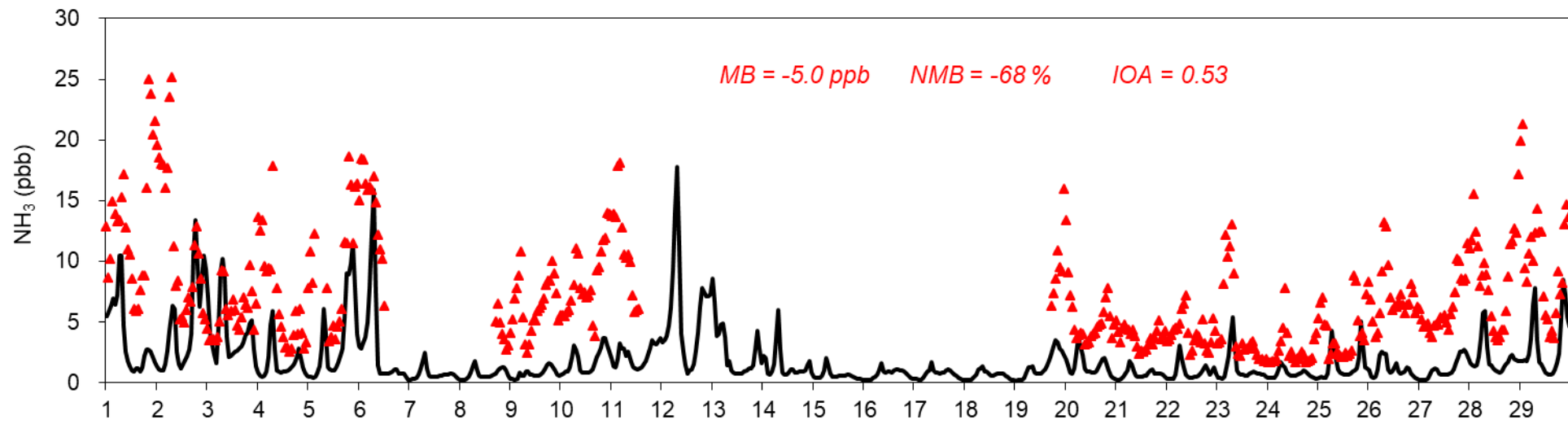
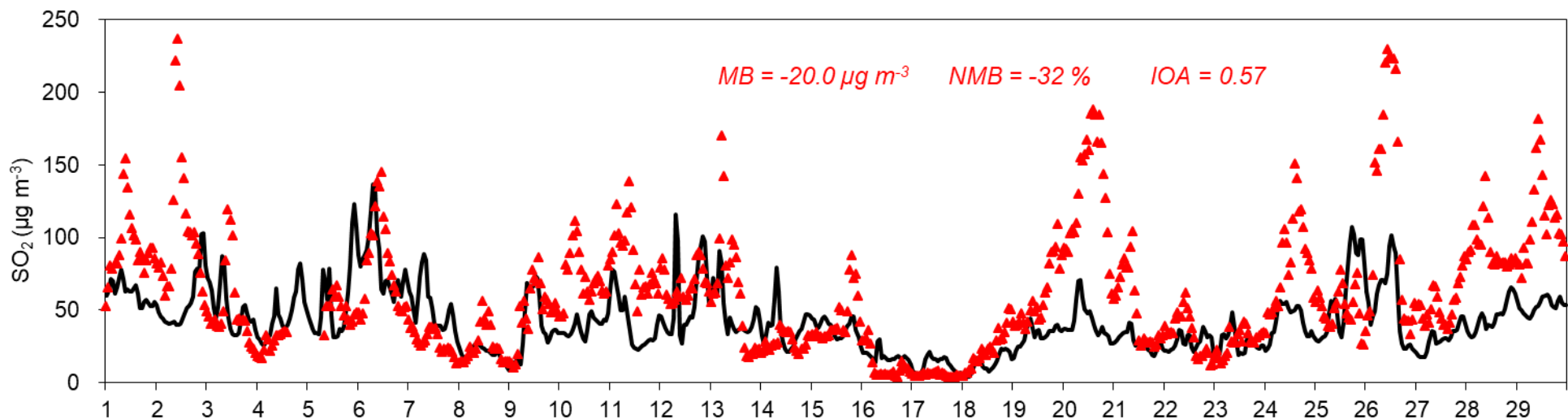
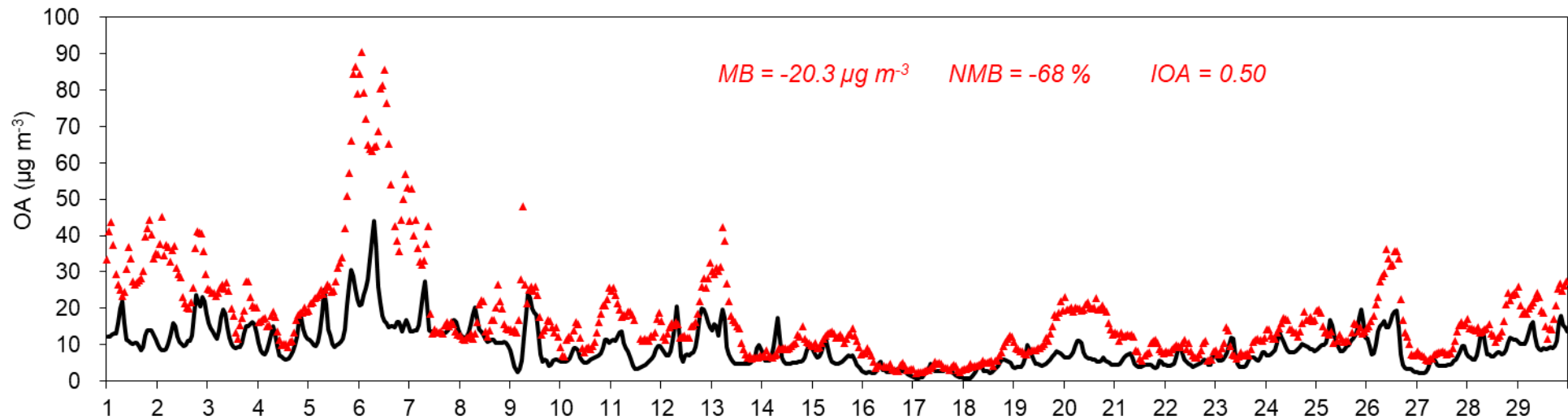


Figure S4. Comparison of observed (black dot-line) and simulated (red dot-line) hourly relative humidity (top row), wind speed (WS, middle row) and temperature (bottom row) at Pudong (left column) and Hongqiao (right column) airport monitoring site.







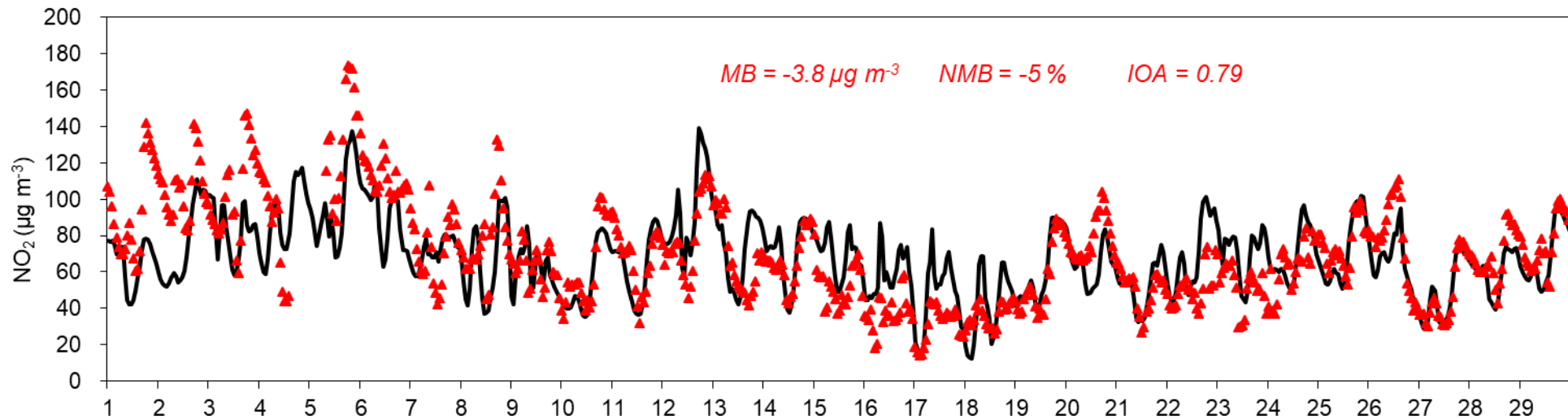


Figure S5. Time series of observed and modeled concentrations for ozone, NH₃, nitrate, ammonium, EC, OA, SO₂ and NO₂ at SAES site during 1 to 29 December 2013

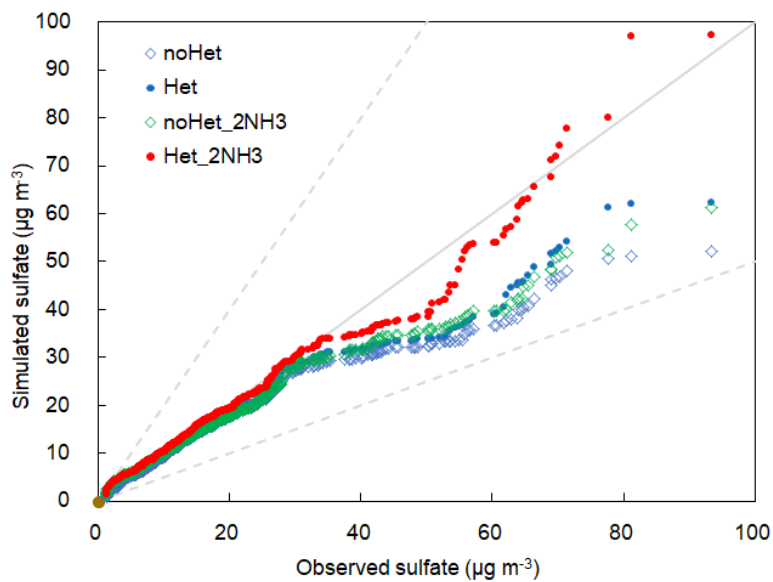


Figure S6: Q-Q (quantile-quantile) plot of simulated hourly sulfate concentrations for different scenarios at SAES site during December 1 to 29, 2013. Solid lines indicate 1:1 lines and dashed lines are 1:2 and 2:1 lines.

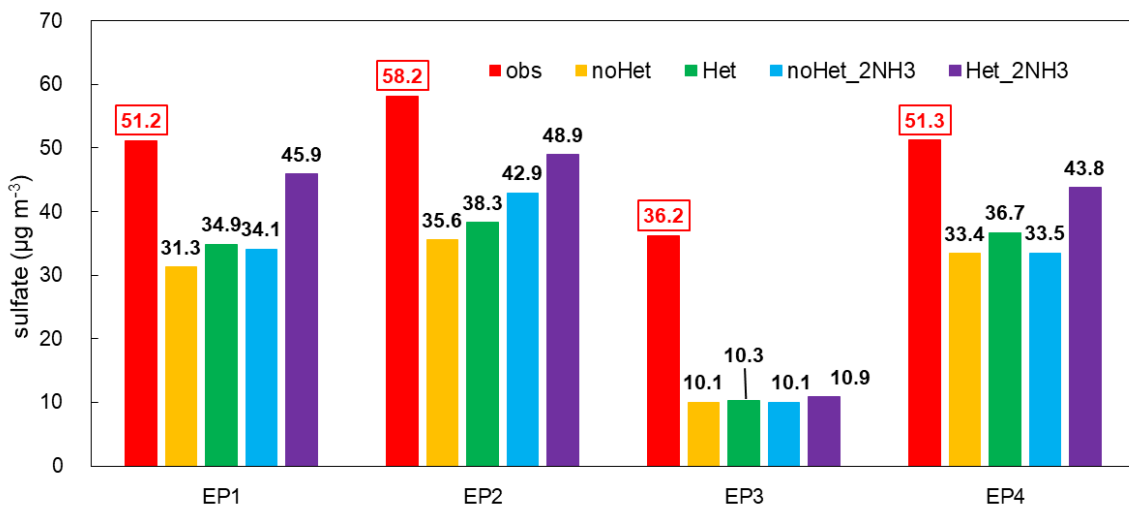


Figure S7. Observed and predicted average sulfate concentrations for four selected heavy haze episodes during 1 to 29 December 2013.

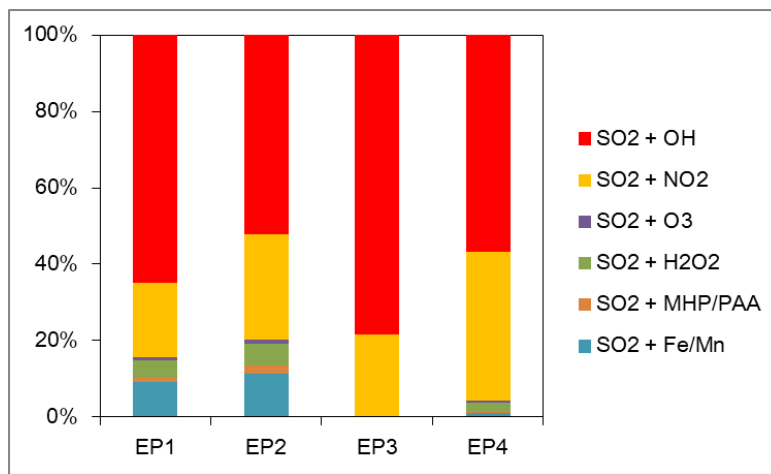


Figure S8. Relative contribution of different sulfate formation pathways to secondary sulfate formation at SAES site during selected pollution episodes

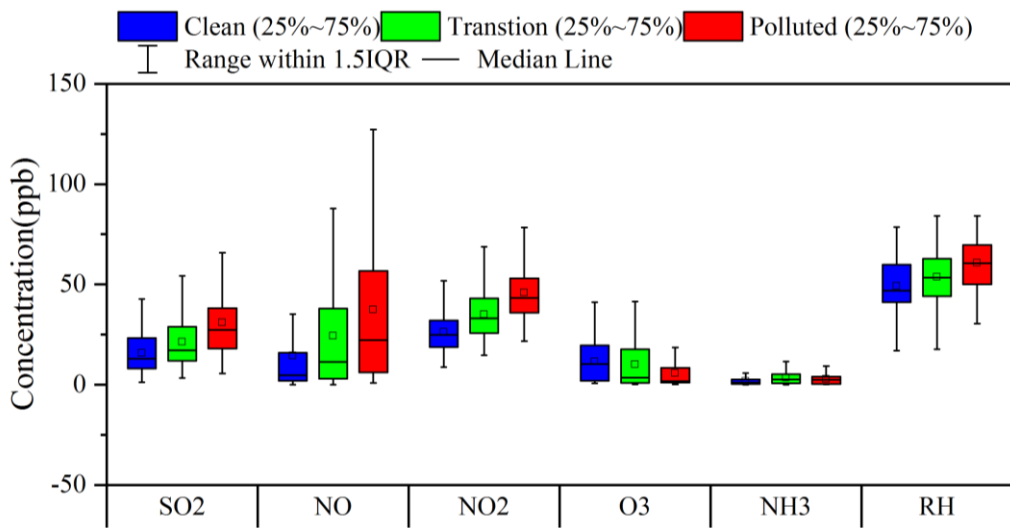


Figure S9. Box and whisker plot of observations by clean, transition and polluted periods during 1 to 29 December 2013 at SAES site.

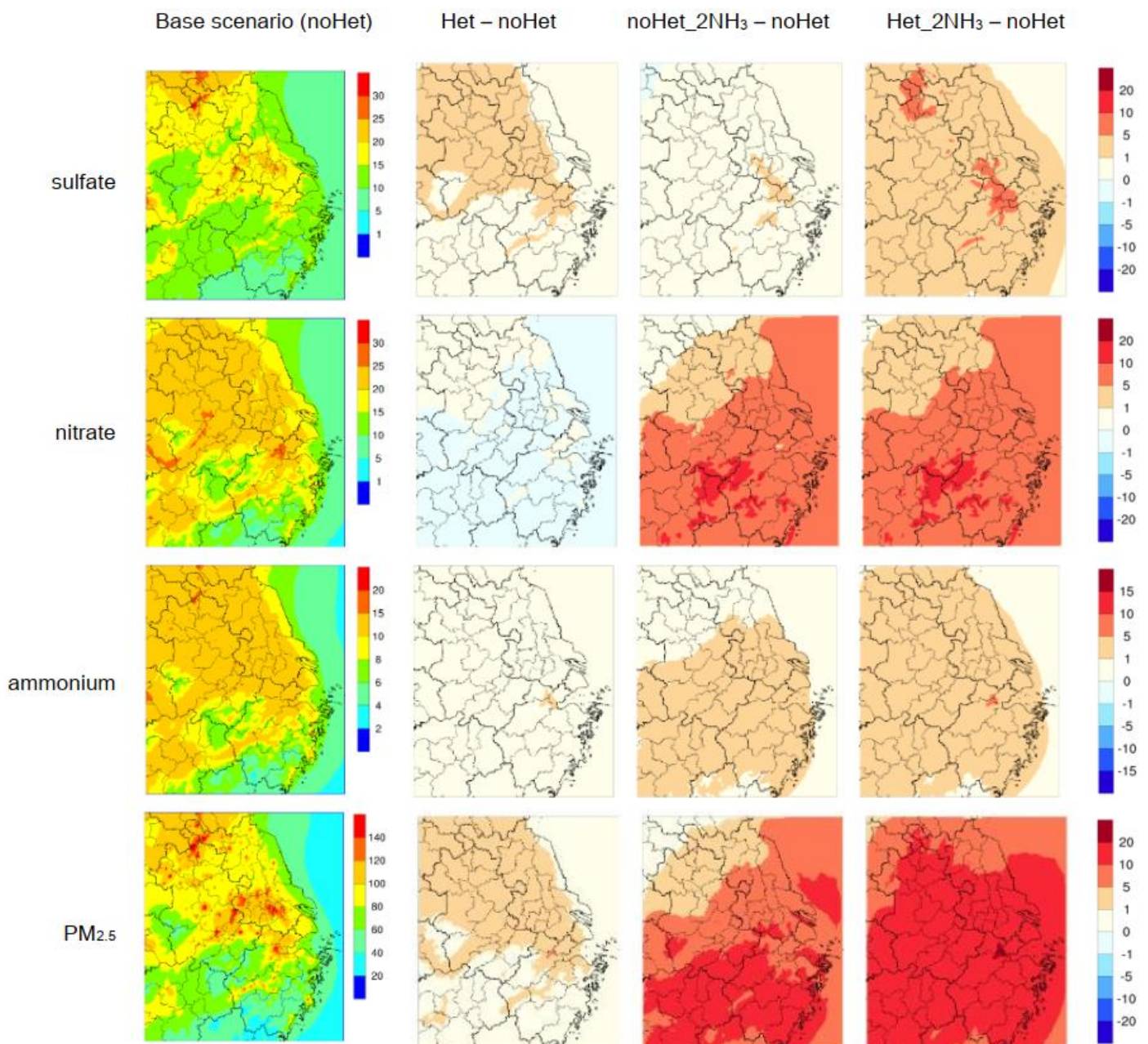


Figure S10: Spatial distribution of simulated monthly average sulfate (first row), nitrate (second row), ammonium and PM_{2.5} (bottom row) in $\mu\text{g m}^{-3}$ over the YRD region for the base case scenario (first column) and the changes between the base case and the other three sensitivity runs: Het (second column), noHet_2NH₃ (third column) and Het_2NH₃ (fourth column).